

*Effect of constitutive heterologous overexpression of E. coli  
NADH insensitive cs gene on the physiology and glucose  
metabolism of P. fluorescens PfO-1*



**CHAPTER 3**

## 3 Chapter 3

### 3.1 INTRODUCTION

Citrate synthase (CS) is a ubiquitous enzyme that catalyzes the first committed step of tricarboxylic acid (TCA) cycle involving condensation of oxaloacetate (OAA) and acetyl-CoA to form citrate. Hence it is the key enzyme governing the carbon flux into the TCA cycle which plays a dual function in the production of cellular energy and biosynthetic precursors under aerobic conditions and only latter under anaerobic conditions, respectively (Park et al., 1994).

#### 3.1.1 Citrate synthase and NADH sensitivity

The CS of gram-negative bacteria are allosteric enzymes designated as type II. Type II CS is a homo-hexamer of identical subunits with monomer size of ~48kDa, and is strongly and specifically inhibited by NADH (Weitzman 1981; Nguyen et al., 2001). *Escherichia coli* and *Acinetobacter anitratum* CS are strongly homologous in amino acid sequence and more distantly resemble the nonallosteric Type I citrate synthase of eucaryotes (Bhayana et al., 1984; Donald et al., 1987; Julie et. al., 2006). *Pseudomonas* CS are also allosteric and their kinetic properties suggest as intermediate between *E. coli* and *A. anitratum* enzymes (Massarini et al., 1975; Higa et al., 1978). Two forms of CS (EC 4.1.3.7) have been found in several species of *Pseudomonas*, a 'large' form (*Mr*~ 1: 250000) which is generally inhibited by NADH and a 'small' form (*Mr*~ 1: 100000) which is insensitive to these nucleotide effectors. Hence the NADH sensitivity of gram negative bacterial CS is attributed to subunit size (**Table 3.1, Fig. 3.1**). A mutant of *Pseudomonas aeruginosa* PAC514 has been found to contain both a 'large' (CSI) and a 'small' (CSII) isozymes (Solomon & Weitzman, 1983; Mitchell et al., 1995).

Table 3.1: Distribution of large and small citrate synthases in *Pseudomonas* species (Coling et al., 1986)

Organism*	RNA homology group	Size of citrate synthase†	Percentage of 'small' citrate synthase‡	
			Gel filtration	FPLC
<i>P. aeruginosa</i> NCIB 8295	I	L + S	14	21
<i>P. aeruginosa</i> 8602		L + S	6	18
<i>P. aeruginosa</i> PAC 514		L + S	90	98
<i>P. aeruginosa</i> PAO 1		L + S	16	NT
<i>P. fluorescens</i>		L + S	25	25
<i>P. putida</i>		L + S	21	22
<i>P. stutzeri</i>		L + S	31	23
<i>P. alcaligenes</i>		S		
<i>P. chlororaphis</i>		S		
<i>P. acidovorans</i>		L		
<i>P. saccharophila</i>	III	S		
<i>P. testosteroni</i>		L		
<i>P. diminuta</i>	IV	L		
<i>P. maltophilia</i>	V	S		

Taxonomic group	Species (code)	Alignment of sequences ( <i>E. coli</i> CS numbering)				No. of identities	NADH inhibition	Size
		105-----116	143-147	156-----169	178-----191			
<b>Alpha subdivision</b>								
Acetobacteraceae	AAC	..NRLINLILLEQ...AFVDP...NRDLAAMLLIAIP...YTOEAFIYRNDL...FARMSLP...				12	-	-
	GRU	- sequence not available -				-	NO	1
	GXY	- sequence not available -				-	NO	1
Caulobacter group	CCR	..HNIYRIVVRAQ...APNSD...ERISAHLLIAAMP...YTVRPFVSRNDL...FAVPADE...				15	-	-
Rhizobiaceae group	RTR	..YRVVHTVVRQ...AFVHD...QRVVASLMIAMP...YHSPFFVYRNDL...FAVPADE...				14	-	-
	SME	..YRVVHTVVRQ...AFVHD...QRVVASLMIAMP...YHSPFFVYRNDL...FAVPADE...				15	-	-
	BJA	..LRVIRHTVVRQ...AFVHD...QRVVASLMIAMP...YHSPFFVYRNDL...FAVPADE...				15	-	-
	NLO	..YRVVHTVVRQ...AFVHD...QRVVASLMIAMP...YHSPFFVYRNDL...FAVPADE...				16	-	-
	NTR	- sequence not available -				-	YES	LARGE
	MEX	..YRVVHTVVRQ...AFVHD...QRVVASLMIAMP...YHSPFFVYRNDL...FAVPADE...				17	NO	LARGE
	MRH	- sequence not available -				-	YES	-
	BHE	..RCTMHTVVRQ...AFVHD...QRVVASLMIAMP...YHSPFFVYRNDL...FAVPADE...				15	-	-
Rhodobacter group	RSP	..YRVVHTVVRQ...AFVHD...QRVVASLMIAMP...YHSPFFVYRNDL...FAVPADE...				16	YES	LARGE
	RCA	..FRIRHTVVRQ...AFVHD...QRVVASLMIAMP...YHSPFFVYRNDL...FAVPADE...				16	YES	-
Rhodospirillaceae	RRU	..KIRVHTVVRQ...AFVHD...QRVVASLMIAMP...YHSPFFVYRNDL...FAVPADE...				16	YES	-
Rickettsiales	RPR	..KKVAHSLVNER...AFVQD...DYDLTAIEMALIP...YHSPFFVYRNDL...FAVPADE...				12	NO	-
	SAR	..RTRVHTVVRQ...AFVHD...HRVSSHLLIAAMP...YHSPFFVYRNDL...FAVPADE...				16	YES	-
<b>Beta subdivision</b>								
Alcaligenaceae	BPE	..SQVIRHTVVRQ...AFVHD...HRVSAIEMALIP...YHSPFFVYRNDL...FAVPADE...				13	-	-
Ammonia-oxidizing	NEU	..DNIKHTVVRQ...AFVHD...HRVSAIEMALIP...YHSPFFVYRNDL...FAVPADE...				16	-	-
Burkholderia group	BPS	..AVVIRHTVVRQ...AFVHD...HRVSAIEMALIP...YHSPFFVYRNDL...FAVPADE...				17	-	-
Neisseriaceae	NME	..NIVRHTVVRQ...AFVQD...HRKAIYLLISIP...YHSPFFVYRNDL...FAVPADE...				16	-	-
	NGO	..NIVRHTVVRQ...AFVQD...HRKAIYLLISIP...YHSPFFVYRNDL...FAVPADE...				16	-	-
	CVI	- sequence not available -				-	YES	-
Ralstonia group	RME	..NSVMHTVVRQ...AFVHD...QRVSAIEMALIP...YHSPFFVYRNDL...FAVPADE...				15	YES	LARGE
<b>Gamma subdivision</b>								
Aeromonadaceae	APU	- sequence not available -				-	YES	LARGE
Alteromonadaceae	SPU	..HVKIRHTVVRQ...AFVQD...HRVIAAYLLVSNMP...YHSPFFVYRNDL...FAVPADE...				16	-	-
Enterobacteriaceae	ECO	..TVVIRHTVVRQ...AFVHD...HRVIAAYLLVSNMP...YHSPFFVYRNDL...FAVPADE...				22	YES	-
	STY	..TVVIRHTVVRQ...AFVHD...HRVIAAYLLVSNMP...YHSPFFVYRNDL...FAVPADE...				22	YES	LARGE
Legionellaceae group	CBU	..RIRKEHTVVRQ...AFVHD...DRVLSAIVLVAAMP...YHSPFFVYRNDL...FAVPADE...				13	NO	-
	LPN	..SLINHTVVRQ...AFVHE...DRVLSAIVLVAAMP...YHSPFFVYRNDL...FAVPADE...				13	-	-
Methylococcaceae	MAL	- sequence not available -				-	NO	-
Moraxellaceae	ACI	..AKVIRHTVVRQ...AFVHN...HRVIAAYLLVSNMP...YHSPFFVYRNDL...FAVPADE...				14	YES	LARGE
Pasturellaceae	PMU	..QLVRHTVVRQ...AFVHD...HRVIAAYLLVSNMP...YHSPFFVYRNDL...FAVPADE...				17	-	-
<b>Pseudomonadaceae</b>	PAE	..GRIKHTVVRQ...AFVHD...HRVSAIEMALIP...YHSPFFVYRNDL...FAVPADE...				15	YES	LARGE
	PPU	..SIVKHTVVRQ...AFVHD...HRVSAIEMALIP...YHSPFFVYRNDL...FAVPADE...				17	YES	LARGE
	AVI	..NNIKHTVVRQ...AFVHD...HRVSAIEMALIP...YHSPFFVYRNDL...FAVPADE...				16	YES	LARGE
Vibrionaceae	VCH	..KIVIRHTVVRQ...AFVHD...HRVIAAYLLVSNMP...YHSPFFVYRNDL...FAVPADE...				18	-	-
Xanthomonas group	XFA	..DEIRHTVVRQ...AFVHD...QRRLAAILIAVY...YHSPFFVYRNDL...FAVPADE...				13	-	-
	XAX	..HEVIRHTVVRQ...AFVHD...QRRLAAILIAVY...YHSPFFVYRNDL...FAVPADE...				13	YES	-
<b>Epsilon subdivision</b>								
Campylobacter group	CJE	..RYEMKKRSFIHE...AFVDP...EYMEMAAIIVAIIP...YHSPFFVYRNDL...FAVPADE...				5	-	-
Helicobacter group	HPY	..EELIRHTVVRQ...AFVHD...DYQTMARIVAIIP...YHSPFFVYRNDL...FAVPADE...				7	NO	-

Figure 3.1: Correlation of Gram-Negative Bacterial Citrate Synthase Subunit Size and NADH Sensitivity with the Presence of NADH-Interacting Residues As Identified in the *E. coli* CS-NADH Complex (Robert et al., 2003)

### 3.1.2 Homology between *E. coli* and *P. fluorescens* citrate synthase

Clustal W multiple alignments show 71% homology between *E. coli* and *P. fluorescens cs* and possess similar regulatory properties. Individual *P. fluorescens* strains also exhibit variations in the coding region of *cs* (Fig. 3.2-3.3)

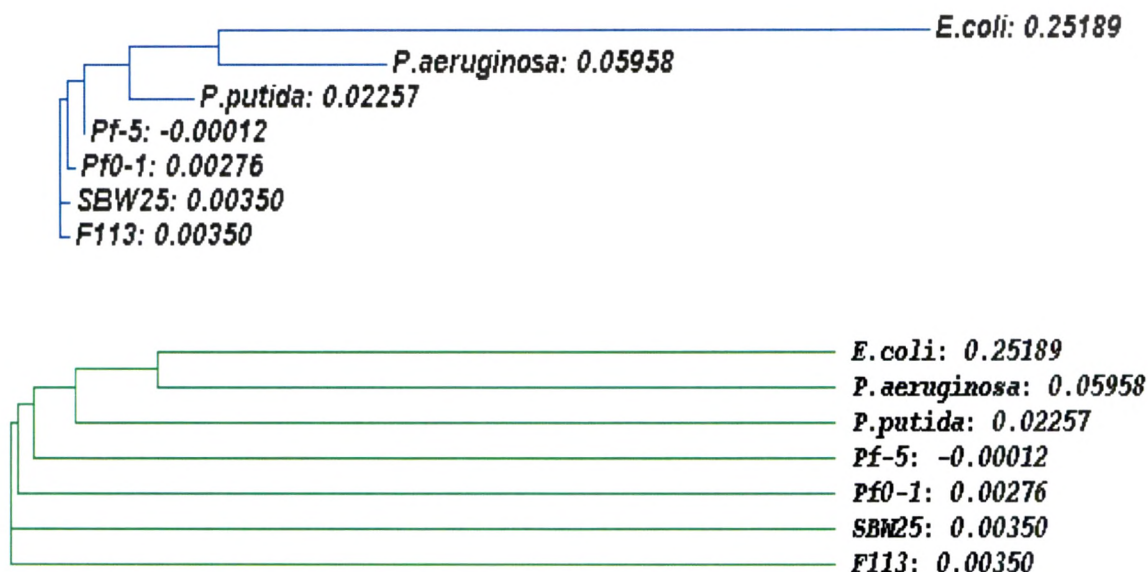


Figure 3.2: Phylogram and cladogram tree

### 3.1.3 Citrate overproduction through citrate synthase overexpression:

The study of the effect of *cs* gene manipulation on citric acid secretion and overall cellular metabolism can have tremendous applications in agriculture. *E. coli* lacking functional *cs* gene failed to utilize glucose unless supplemented with glutamate (or other TCA cycle intermediates) and had reduced growth as compared to the wild type (Vandedrinck et al., 2001; De Maeseneire et al., 2006). On the other hand, *cs* gene overexpression or underexpression in *E. coli* had no effect on growth on glucose while on acetate as sole carbon source; CS levels strongly affected the growth rate (Vandedrinck et al., 2001). Transgenic tobacco plants overexpressing *Pseudomonas aeruginosa cs* gene under the control of CaMV promoter increased excretion of citrate (Bucio et al., 2000). These citrate secreting plants enhanced the P solubilization efficiency and yielded more leaf and fruit biomass when grown under P-limiting conditions.

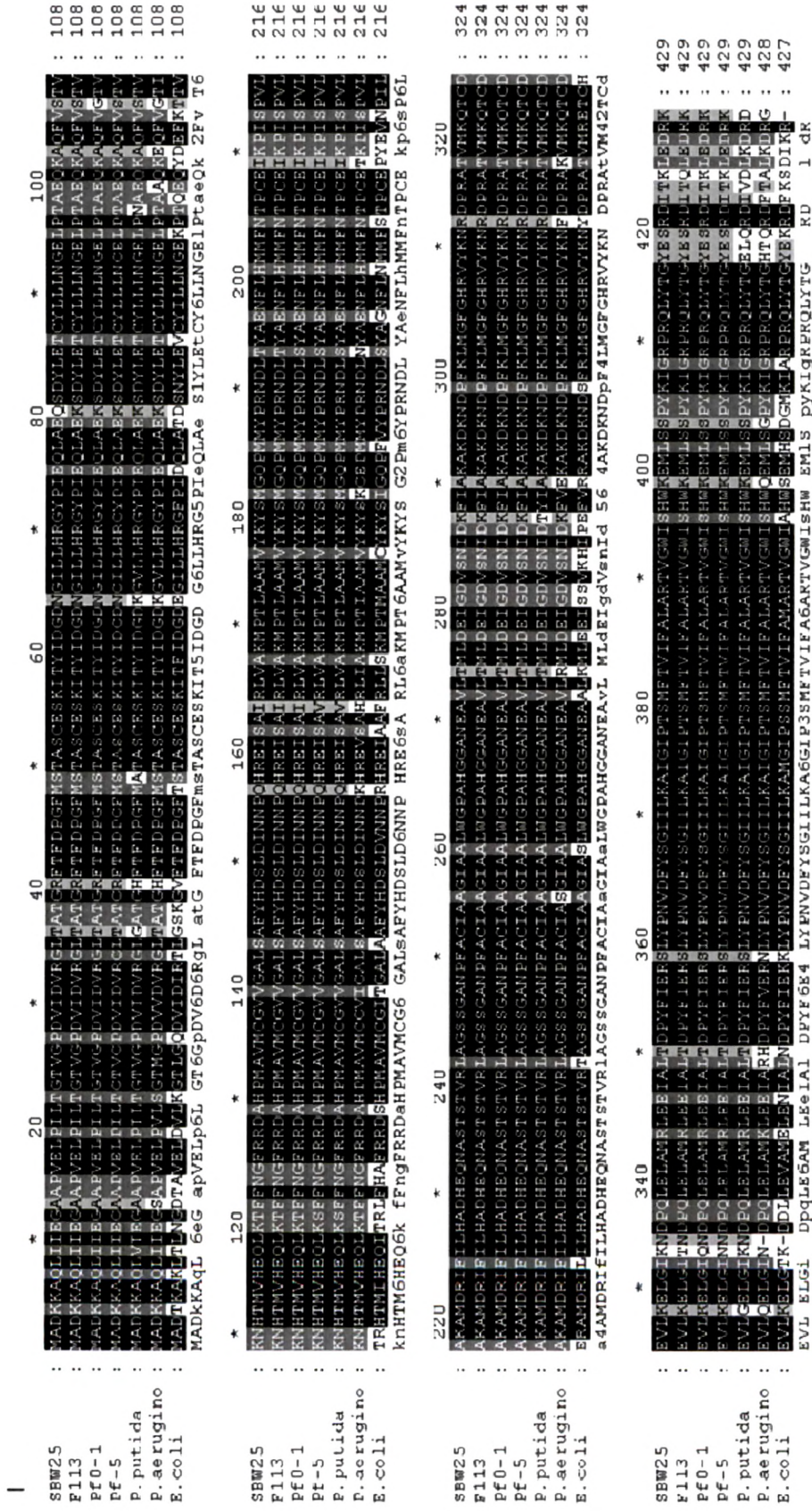


Figure 3.3: CS homology by ClustalW analysis between *E. coli* and fluorescent pseudomonads. Enclosed black areas indicate identical amino acid residues.

Overexpression of mitochondrial citrate synthase in *Arabidopsis thaliana* improved growth on a phosphorus-limited soil and improved the growth of carrot cells on Al-phosphate medium; the effect suspected to be due to enhanced secretion of citric acid (Koyama et al., 1999; 2000). Similar studies in *Nicotiana benthamiana* elicited Al induced citrate excretion (Deng et al., 2009) and conferred Al-tolerance in *S. cerevisiae* and canola (*Brassica napus cv Westar*) (Anoop et al, 2003). However, up to 11-fold overproduction of CS did not increase the rate of citric acid production by *Aspergillus niger*, suggesting that citrate synthase contributes little to flux control in the pathway involved in citric acid biosynthesis by the strain (Ruijter et al., 2000). On the other hand, *E. coli* K and B isocitrate dehydrogenase (*icd*) mutants accumulated high levels of citrate when grown on glucose with a concomitant increase in CS activity upto more than 2 fold (Lakshmi and Helling, 1976; Aoshima et al., 2003). Similarly, *B. subtilis icd* mutant in early stationary phase accumulated ~15 fold higher intracellular citrate levels as compared to the wild type (Matsuno et al., 1999). *gltA* gene overexpression in *E. coli* increased the maximum cell dry weight by 23% and reduced acetate secretion (De Maeseneire et al., 2006).

Metabolic studies in *E. coli* demonstrated that high citric acid yields could be attained on glucose and depending on the host metabolism; glucose transport, flux through catabolic pathways and the regulatory mechanisms influenced by intracellular metabolite pools appear to facilitate the citrate accumulation (Elias, 2009). Overexpression of *Escherichia coli* citrate synthase (*gltA*) gene in *Pseudomonas fluorescens* ATCC 13625 yielded intracellular and extracellular citric acid levels during the stationary phase, respectively (Koch et al., 2005). It was also postulated that increasing CS activity in *P. fluorescens* for citric acid overproduction from glucose is a better strategy than *icd* mutation in *E. coli*, which reduces biomass and growth (Aoshima et al., 2003). The amount of citric acid produced by *P. fluorescens* overexpressing *E. coli cs* gene was similar to that secreted by the phosphate solubilizing *Bacillus coagulans* and *Citrobacter koseri* on glucose (Gyaneshwar et al., 1998). But the amount of citric acid secreted by this approach is insufficient for effective P solubilization in field condition. Hence further strategies are required to increase the citrate level.

### 3.1.4 Rational of the present study

Functional properties of nine sequence variants of *E. coli* CS at NADH binding site had had varied inhibition in kinetic parameters for catalysis (Fig. 3.5) (Stockell et al., 2003). In three cases, Y145A, R163L, and K167A, NADH inhibition has become extremely weak (Table 3.2, Fig. 3.4).

```

MADTKAKLTL NGDTAVELDV LKGTLGQDVI DIRTLGSKGV
FTFDPGFTST ASCESKITFI DGDEGILLHR GFPIDQLATD
SNYLEVCYIL LNGEKPTQEQ YDEFKTTVTR HTMIHEQITR

145pyrophosphate (NADH)
LFHAFRRDSH PMAVMCGITG ALAAFYHDSL DVNNPRHREI
163 and 167 pyrophosphate (NADH)
AAFRLLSKMP TMAAMCYKYS IGQPFVYPRN DLSYAGNFLN
207/208 NADH
MMFSTPCEPY EVNPILERAM DRILILHADH EQNASTSTVR
TAGSSGANPF ACIAAGIASL WGPAHGGANE AALKMLEEIS

306activesite
SVKHIPEFVR RAKDKNDSFR LMGFGHRVYK NYDPRATVMR
ETCHEVLKEL GTKDDLLEVA MELENIALND PYFIEKKLYP
363 active site
NVDFYSGIIL KAMGIPSSMF TVIFAMARTV GWIAHWSEMH
SDGMKIARPR QLYTGYEKRD FKSDIKR 427

```

Figure 3.4: *E. coli* cs protein sequence showing the regulatory variants

Table 3.2: NADH binding and inhibition by variant citrate synthases (Stokell et al., 2003)

Variant	K <sub>d</sub> (μM)	K <sub>i</sub> (μM)	Maximum inhibition(%)
Wild type	1.6±0.1	2.8±0.4	100±10
R109L	1.16±0.04	1.7±0.2	96±6
H110A	5.2±0.2	121±11	97±3
T111A	6.6±0.2	80±15	87±6
Y145F	>100	790±210	100±3
R163L	5.81±0.04	400±80	77±8
K167A	4.1±0.2	630±130	100±10
Q128A	6.1±0.5	18±3	100±7
N189A	6.9±0.8	242±26	96±5
T204A	10.2±0.4	165±36	100±7

The present study demonstrates the effect of overexpression of NADH insensitive *cs* variants e.g., Y145F, R163L, and K167A on citric acid accumulation and secretion by *P. fluorescens* PfO-1.

## 3.2 WORK PLAN

The experimental plan of work includes the following-

### 3.2.1 Bacterial strains used in this study

**Table 3.3: List of bacterial strains used.**

Bacterial strains	Characteristics	Source/Reference
<i>E. coli</i> DH5 $\alpha$	F- $\phi$ 80 $\Delta$ lacZ $\Delta$ M15 $\Delta$ (lacZYA-argF) U169 <i>recA1 endA1 hsdR17</i> (rk-, mk+) <i>phoA supE44 <math>\lambda</math>-thi-1 gyrA96 relA1</i>	Sambrook and Russell,2001
<i>E. coli</i> W620	<i>cs</i> mutant strain exhibiting glutamate auxotrophy, CGSC 4278 - <i>glnV44 gltA6 galK30</i> <i>LAM-pyrD36 relA1 rpsL129 thi-1</i> ; Str	<i>E. coli</i> Genetic Stock Center
<i>P. fluorescens</i> PfO-1	Wild type strain	
<i>Pf</i> (pAB8)	<i>P. fluorescens</i> PfO-1 with pAB8; Km <sup>r</sup>	This study
<i>Pf</i> (pAB7)	<i>P. fluorescens</i> PfO-1 with pAB7; Km <sup>r</sup>	This study
<i>Pf</i> (pR163L)	<i>P. fluorescens</i> PfO-1 with pR163L; Km <sup>r</sup>	This study
<i>Pf</i> (pK167A)	<i>P. fluorescens</i> PfO-1 with pK167A; Km <sup>r</sup>	This study
<i>Pf</i> (pY145F)	<i>P. fluorescens</i> PfO-1 with pY145F; Km <sup>r</sup>	This study

Detailed characteristics of these strains and plasmids are given in **Section 2.1** Parent strains and the transformants of *E. coli* and *Pseudomonas fluorescens* were respectively grown at 37°C and 30°C with streptomycin and kanamycin as and when required, at final concentrations varying for rich and minimal media as described in **Section 2.2, Table 2.4**

### 3.2.2 Cloning and expression of NADH insensitive *E. coli cs* gene in *P. fluorescens* Pfo-1

The strategy for construction of recombinant *P. fluorescens* strain harbouring NADH insensitive *cs* gene are depicted in Fig. 3.5.

#### 3.2.2.1 Construction of *Pseudomonas* stable plasmid containing *E. coli* NADH insensitive *cs* gene under *lac* promoter

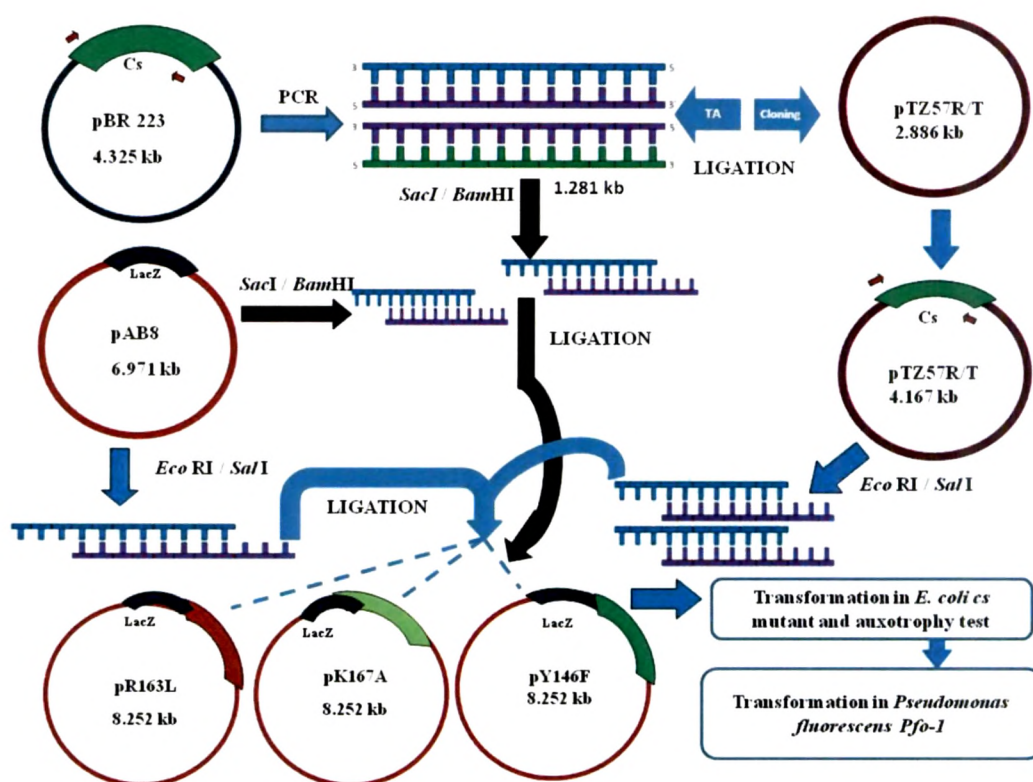


Figure 3.5: Schematic representation of construction of pseudomonad stable vectors containing NADH insensitive *E. coli cs* gene under *lac* promoter. Blue arrows indicate strategy1 and black arrow indicate strategy 2

### 3.2.2.1.1 Incorporation of NADH insensitive *E. coli* *cs* in pUCPM18:

PCR amplification of pBR322 plasmid containing NADH insensitive *E. coli* *cs* (*gltA*) gene are carried out using gene specific primer (Table 3.4) to get an amplification of 1281 bp each of *R163L*, *K167A*, *Y145F*

**Table 3.4:** NADH insensitive *cs* primers

Primer	Oligonucleotide Sequence(5'-3'end)	Tm/GC%
<b>EcCSApaI SacIF</b>	5' <u>CGAGCTCGGGCCCTTTTTCACGGAGGAAACC</u> <u>ACAATG GCT GAT ACA AAA GC</u>	59.6°C, 52.2%
<b>EcCSKpnIBamHIR</b>	<u>CGGGATTCCGGATCC</u> G TTA ACG CTT GAT ATC GC	59.6°C, 46.2%

**SacI ApaI:** CGAGCTCGGGCCC **KpnI BamHI:** GGGGTACC CGGATCCG

**RBS:** 5'CACGGAGGAATCAACT 3'

Cloning of the isolated *cs* gene was carried out in broad host range cloning vector pUCPM18 having kanamycin resistance gene using two strategies. In one strategy the amplified 1281 bp gene was directly cloned into pUCPM18  $km^r$  vector in SacI/BamHI site under *lac* promoter. In another strategy the amplified product was cloned into pTZ57R using InsT/Aclone™ PCR product cloning kit, MBI Fermentas and transformed into *E. coli* DH5 $\alpha$ . The presence of the appropriate plasmid was checked by PCR and restriction enzyme digestion and subcloned into pUCPM18  $kan^r$  vector in *EcoRI/SalI* restriction site (**Fig.3.6**)

### 3.2.2.1.2 Functional confirmation of CS expressed from pR163L, pK167A and pY145F

*E. coli* W620, which exhibited glutamate auxotrophy due to mutation in *cs* gene, was used to determine the functionality of the *cs* gene. pAB7, pR163L, pK167A and pY145F along with the respective controls pAB8 plasmids were transformed into *E. coli* W620 (**Table 2.1, Section 2.2**). The transformants were selected on agar plates with streptomycin and kanamycin (doses as recommended in **Section 2.2**) and confirmed the presence of

respective plasmids. Subsequently these were subjected to auxotrophy complementation studies (Section 2.6).

### 3.2.2.1.3 Development of *P. fluorescens* PfO-1 harboring NADH insensitive *E. coli cs* gene

The recombinant plasmids pR163L, pK167A and pY145F along with control pAB8 and plasmid containing wild type *cs* gene pAB7 were transformed by electroporation in *P. fluorescens* PfO-1 (Section 5.2.2). The transformants were selected on pseudomonas agar plate containing kanamycin and were confirmed by fluorescence and restriction enzyme digestion of the isolated plasmids from the respective strains (Section 2.4.5).

### 3.2.3 Effect of NADH insensitive *E. coli cs* gene expression on the physiology and glucose metabolism of *P. fluorescens* PfO-1.

*P. fluorescens* PfO-1 transformants were subjected to physiological experiments involving growth and organic acid production profiles on M9 minimal medium with 100mM glucose as carbon source. The samples withdrawn at regular interval were analyzed for O.D.600nm, pH, and extracellular glucose (Section 2.7.2). Stationary phase cultures harvested at the time of pH drop were subjected to organic acid estimation using HPLC (Section 2.7.3). The physiological parameters were calculated as in section 2.7.3. The enzyme assays were performed as described in 2.8, with CS, G-6-PDH, ICDH, PYC being assayed in both mid-log to late-log and stationary phase cultures while ICL and GDH are being assayed in the mid log and stationary phase cultures respectively.

## 3.3 RESULTS

### 3.3.1 Construction of *Pseudomonas* stable plasmid containing NADH insensitive *E. coli cs* gene under *lac* promoter

The plasmids pR163L, pK167A and pY145F containing *E. coli* NADH insensitive *cs* gene *r163l*, *k16a* and *y146f* respectively under *lac* promoter of pUCPM18 plasmid with *km<sup>r</sup>* gene were constructed in a two step cloning procedure schematically represented and discussed in section (Fig. 3.6). All plasmids were confirmed based on restriction digestion pattern (Fig. 3.7-3.14) and PCR (Fig. 3.15). The plasmids pAB8 and pAB7 were taken as a control for all the experiments.



Figure 3.6: PCR amplification of NADH insensitive *cs* gene. *R163L* (Lane1), *K167A* (Lane2), *Y145F* (Lane3); *pCCgltA* (Lane4), *pESgltA* (Lane5) each of 1281 bp

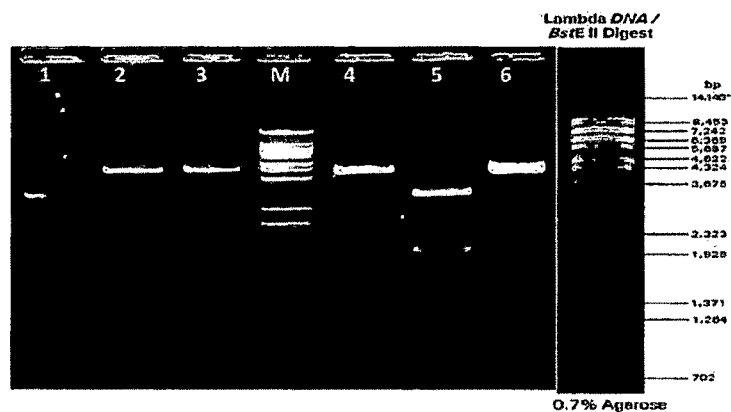


Figure 3.7: Restriction digestion pattern of pTZ57R/T *Y146F* clone with *SacI*. Lane1, 5: plasmid with *Y145F* gene in right orientation (2886 bp and 1281 bp). Lane 2, 3, 4, 6: plasmid with *Y145F* in opposite orientation (4167 bp). Lane M: Molecular weight marker (MWM)-Lambda DNA cut with *BstEII*

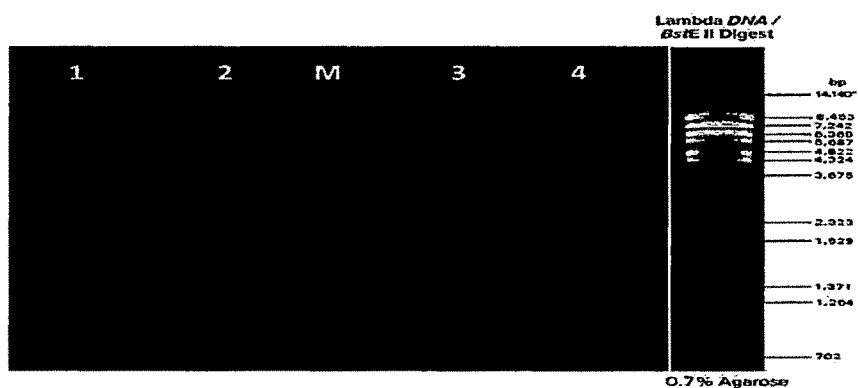
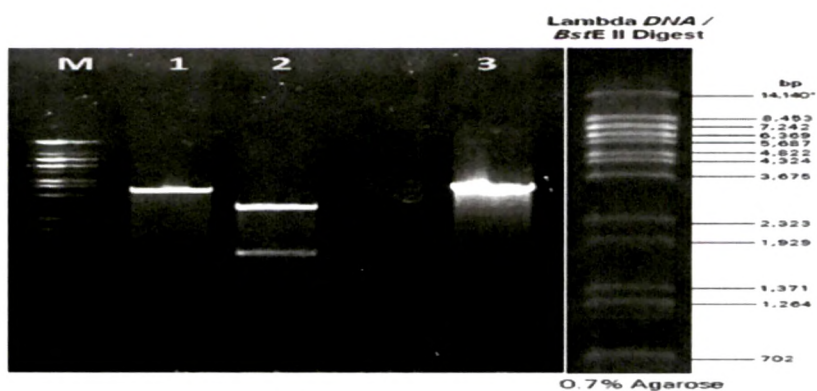
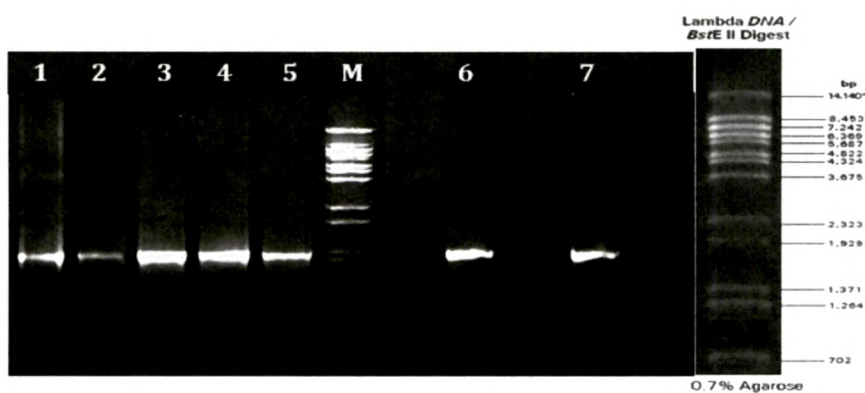


Figure 3.8: Restriction digestion pattern of pTZ57R/T *K167A* clone . Lane1-Lane4: pTZ57R/T *K167A* plasmid digested with *KpnI*(2886 bp and 1281 bp) . Lane M: Molecular weight marker(MWM)-Lambda DNA cut with *BstEII*



**Figure 3.9: Restriction digestion pattern of pTZ57R/T *R146L* clone with *KpnI*.** Lane1, 3: plasmid containing gene in opposite orientation (4167 bp). Lane 2: plasmid containing gene in right orientation (2886 bp and 1281 bp). Lane M: Molecular weight marker(MWM)-Lamda DNA cut with *BstEII*



**Figure 3.10: PCR amplification of TA clones.** Lane1, 2: *R163L*; Lane3, 4:*Y145F*; Lane5, 6: *K167A* Lane7: wild type *cs* gene each gene of 1281 bp; Lane M: Molecular weight marker (MWM)-Lamda DNA cut with *BstEII*.

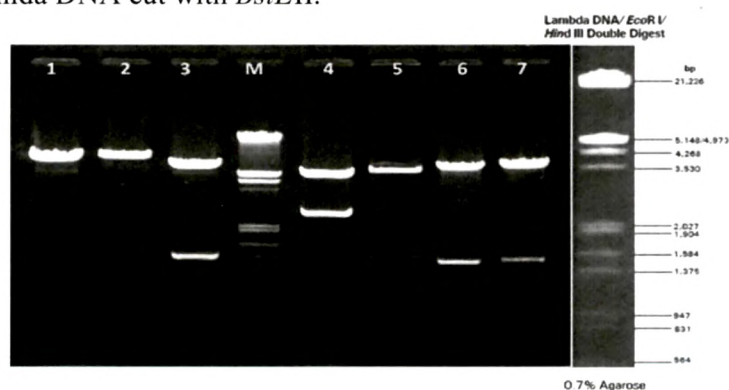


**Figure 3.11: Restriction digestion pattern for pY145F.** Lane1: pY145F linearizes with *SacI* (8252bp); Lane2: pY145F linearizes with *BamHI* (8252 bp); Lane3: pY145F digested with *EcoRI-SalI* (6971bp,1281bp); Lane4: pY145F digested with *EcoRI-BglII*(6971bp,2918 bp);Lane5: pAB8 digested with *EcoRI-BglII*

(5334bp,1637 bp); Lane6:pY145F digested with *ApaI* (6971 bp,1281 bp); Lane6: pY145F digested with *KpnI* (6971 bp,1281 bp); LaneM:MWM with Lamda DNA *EcoRI/HindIII* double digest.

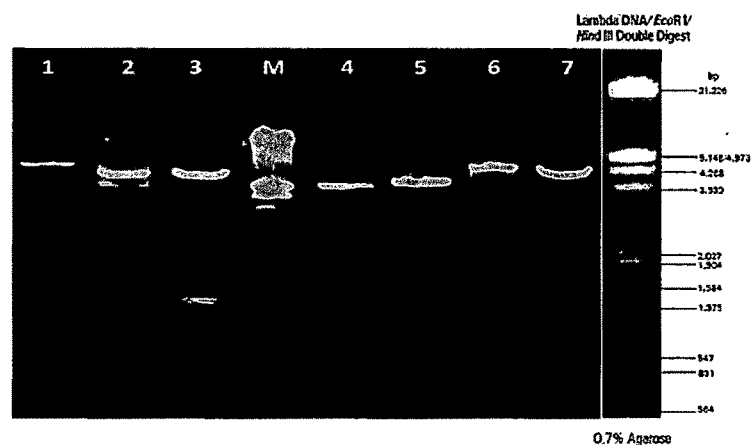


**Figure 3.12: Restriction digestion pattern for pK167A.** Lane1: pK167A plasmid linearized with *BamHI* (8252bp); Lane2: pK167A digested with *ApaI* (6971bp, 1281bp); Lane3: pK167A digested with *EcoRI-Sall*(6971bp,1281bp);Lane4: pK167A digested with *EcoRI-BglIII* (5334bp,2918 bp); lane5:pAB8 digested with *EcoRI-BglIII* (5550bp,1421bp); lane6: pK167A plasmid linearized with *SacI* (8252bp); Lane7: pK167A plasmid linearized with *EcoRI* (8252bp); laneM: MWM lamda DNA *EcoRI/HindIII* double digest

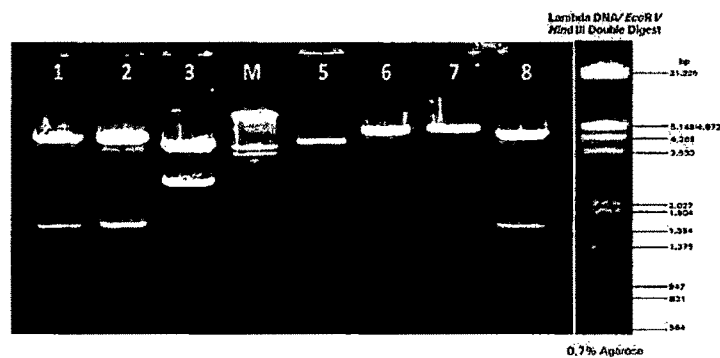


**Figure 3.13: Restriction digestion pattern for pR163L.** Lane1: pR163L digested with *KpnI* (6971bp,1281bp); Lane2: pR163L digested with *EcoRI-Sall* (6971bp,1281bp); Lane3: pR163L digested with *EcoRI-BglIII*(5334bp,2918 bp); Lane5: pAB8 digested with *EcoRI-BglIII* (5550bp,1421bp); lane6: pR163L linearized with *ApaI*(8252bp); lane7: pR163L linearized with *SacI*(8252bp) ; Lane8: pR163L digested with *EcoRI* (6971bp,1281bp); laneM: MWM lamda DNA *EcoRI/HindIII* double digest

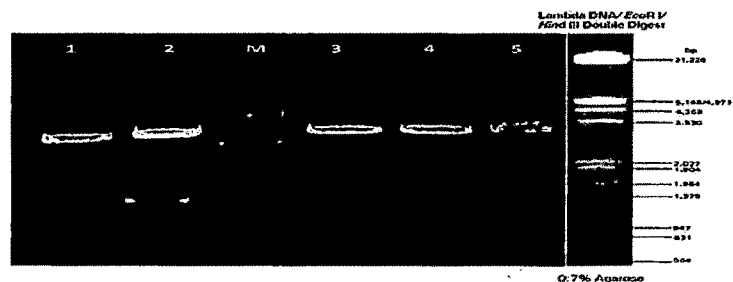


**Figure 3.14:** Restriction digestion pattern for pUCPM18 Km<sup>r</sup> containing NADH insensitive *cs* gene digested with EcoRI-BamHI (StrategyII). Lane1,Lane2: pY145F (6971bp,1281bp); Lane3: pR163L ((6971bp,1281bp); Lane4: pK167A (6971bp,1281bp); Lane5: pAB8 (6971bp,1281bp);LaneM: MWM containing LambdaDNA EcoRI-HindIII double digest.

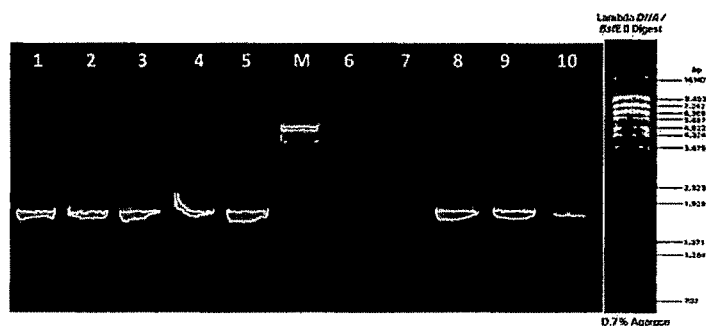


**Figure 3.15:** PCR amplification of NADH insensitive gene cloned in pUCPM18 km<sup>r</sup> vector. Lane1-Lane3: pUCPM18 Km<sup>r</sup> containing Y145F gene; Lane4,5: pUCPM18 Km<sup>r</sup> containing R163L gene; Lane6-Lane10:pUCPM18 Km<sup>r</sup> containing K167 gene;each gene of 1281bp;LaneM: MWM containing lambda DNA cut with BstEII.

### 3.3.2 *E. coli cs* mutant complementation

*E. coli cs* mutant strain harboring pAB7, pR163L, K167A and pY145F could grow on M9 minimal medium containing glucose as carbon source or when induced with 0.1mM IPTG without glutamate supplementation unlike the controls pAB8 (Fig.3.16).



**Figure 3.16: Complementation of *E. coli* W620 mutant phenotype by wild type and NADH insensitive *cs* plasmids.** a: *E. coli* W620-deletion mutant of *cs* gene b: *E. coli* W620 with pAB8 plasmid c: *E. coli* W620 with pAB7 plasmid d: *E. coli* W620 with pR163L plasmid e: *E. coli* W620 with pK167 plasmid f: *E. coli* W620 with pY145F plasmid. All plasmid bearing strains are induced with 0.1mM IPTG. Growth is monitored on M9 medium with 0.2% glucose (Section ) +/- at the corners of each image indicates absence and presence of 340µg/ml glutamate in the medium, respectively.

### 3.3.3 Partial sequencing of pY145F plasmid

Partial sequencing of the PCR product amplified from pY146F plasmid when analysed using NCBI BLAST (Basic Local Alignment Search Tool) and Ribosomal Database Project (RDP) II, online homology search programs, revealed maximum identity (99%) to *E. coli* citrate synthase (GenBank Accession number AAA23892) (Fig. 3.17-3.18).

#### >YFPCRPRODUCT\_YFFOR\_S702

```
CNCNNANCGGCACCCTGAACGGGGATACAGCTGTTGAACTGGATGTGCTGAAAGGCACGC
TGGGTCAAGATGTTATTGATATCCGTACTCTCGGTTCAAAGGTGTGTTCACCTTTGACC
CAGGCTTCACTTCAACCGCATCCTGCGAATCTAAAATTACTTTTATTGATGGTGATGAAG
GTATTTTGCTGCACCGCGGTTTCCCGATCGATCAGCTGGCGACCGATTCTAACTACCTGG
AAGTTTGTTACATCCTGCTGAATGGTGA AAAAACC GACTCAGGAACAGTATGACGAATTTA
AAACTACGGTGACCCGT CATACCATGATCCACGAGCAGATTACCCGTCTGTTCCATGCTT
TCCGTCGCGACTCGCATCCAATGGCAGTCATGTGTGGTATTACCGGCGCGCTGGCGGCGT
TCTTTCACGACTCGCTGGATGTTAACAATCCTCGTCACCGTGAAATTGCCGCGTTCCGCC
TGCTGTCGAAAATGCCGACCATGGCCGCGATGTGTTACAAGTATTCATTGGTCAGCCAT
TTGTTTACCAGCGCAACGATCTCTCCTACGCCGGTAACTTCTGAATATGATGTTCTCCA
CGCCGTGCGAACCGTATGAAGTTAATCCGATTCTGGAACGTGCTATGGACCGTATTCTGA
TCCTGCACGCTGACCATGAACAGAACGCCTCTACCTCCACCGTGCGTACCGCTGGCTCTT
```

CGGGTGC GAACCCGTTTGCCTGTATCGCAGCAGGTATTGCTTCACTGTGGGGACCTGCGC  
 ACGGCGGTGCTAACGAAGCGGCGCTGAAAATGCTGGAAAGAAATCAGCTCCGTTAAACACA  
 TTCCGGAAATTTGTTTCGTTCGTGCGAAAGACAAAAATGATTCTTTCCGCCTGATGGGCTTCG  
 GTCACCGCGTGTACAAAATTACGACCCGCGCGCCACCGTAATGCGTGAAACCTGCCATGA  
 AGTGCTGAAAGAGCTGGGCACGAANNTGACCTGCTGNAGT

Figure 3.17: Partial sequence of *E. coli* NADH insensitive *cs* gene

```
>gb|U00096.2|Escherichia coli str. K-12 substr. MG1655, complete genome
Length=4639675

Features in this part of subject sequence:
  citrate synthase

Score = 1777 bits (962), Expect = 0.0
Identities = 971/975 (99%), Gaps = 1/975 (0%)
Strand=Plus/Minus

Query 4      CACCCCTGACCGGGGATACAGCTGTTGAACTGGATGIGCTGAAAGGCACGCTGGGTCAGA 63
             |||||
Sbjct 753668  CACCCCTCACCGGGGATACAGCTGTTGAACTGGATGIGCTGAAAGGCACGCTGGGTCAGA 753609

Query 64     TGTATTGATATCCGTAICTCTCGGTTCAAAGGTGTGTTACCTTTGACCCAGGCTTCAC 123
             |||||
Sbjct 753608  TGTATTGATATCCGTAICTCTCGGTTCAAAGGTGTGTTACCTTTGACCCAGGCTTCAC 753549

Query 124    TTCAACCGCATCCTGCGAATCTAAAATTACTTTTATTGATGGTGTGTAAGGTATTTTGT 183
             |||||
Sbjct 753548  TTCAACCGCATCCTGCGAATCTAAAATTACTTTTATTGATGGTGTGTAAGGTATTTTGT 753489

Query 184    GCACCGCGGTTTCCCGATCGATCAGCTGGCGACCGATTCTAACTACCTGGAGTTTGTTA 243
             |||||
Sbjct 753488  GCACCGCGGTTTCCCGATCGATCAGCTGGCGACCGATTCTAACTACCTGGAGTTTGTTA 753429

Query 244    CATCCTGCTGAATGGTGAAAAACCGACTCAGGAACAGTATGACGAATTTAAACTACGGT 303
             |||||
Sbjct 753428  CATCCTGCTGAATGGTGAAAAACCGACTCAGGAACAGTATGACGAATTTAAACTACGGT 753369

Query 304    GACCCGTCATACCATGATCCACGAGCAGATTACCCGTCGTTCATGCTTTCCGTCGCGA 363
             |||||
Sbjct 753368  GACCCGTCATACCATGATCCACGAGCAGATTACCCGTCGTTCATGCTTTCCGTCGCGA 753309

Query 364    CTCGCATCCRAATGGCAGTCAITGTTGGTATTACCGGCGCGCTGGCGGCGTTCTTTCACGA 423
             |||||
Sbjct 753308  CTCGCATCCRAATGGCAGTCAITGTTGGTATTACCGGCGCGCTGGCGGCGTTCTTTCACGA 753249

Query 424    CTCGCTGGATGTTAACAACTCTCGTCACCGTGAAATGCGCGGTTCCGCCTGCTGTGAA 483
             |||||
Sbjct 753248  CTCGCTGGATGTTAACAACTCTCGTCACCGTGAAATGCGCGGTTCCGCCTGCTGTGAA 753189

Query 484    AATGCCGACCAATGGCCGCGAIGTGTACAGTATTCCATTGGICAGCCATTTGTTTACCA 543
             |||||
Sbjct 753188  AATGCCGACCAATGGCCGCGAIGTGTACAGTATTCCATTGGICAGCCATTTGTTTACCA 753129

Query 544    GCGCAACGATCTCTCCTACGCGGTAACCTTCTGAAATATGATGTTCTCCACGCGGTGCGA 603
             |||||
Sbjct 753128  GCGCAACGATCTCTCCTACGCGGTAACCTTCTGAAATATGATGTTCTCCACGCGGTGCGA 753069

Query 604    ACCGTATGAAGTTAATCCGATTCTGGACGCTGCTATGGACCGTATTCTGATCCIGCACGC 663
             |||||
Sbjct 753068  ACCGTATGAAGTTAATCCGATTCTGGACGCTGCTATGGACCGTATTCTGATCCIGCACGC 753009
```

Figure 3.18 : NCBI BLAST analysis of partial *cs* sequence

Pairwise alignment of the sequence with original *E. coli* K12 NADH sensitive *cs* sequence from database using EBI pairwise alignment tool, revealed a mutation of tyrosine residues in 146 amino acid position to phenylalanine (**Fig. 3.19**).

PCR	1	-----CNCNNANCGGCACCCCTGAACGGGGATACAGCTGTTG	36
ORIGINAL	1	atggctgatacaaaagcaaac-tcaccctcaacggggatcacagctgttg	49
PCR	37	AACTGGATGTGCTGAAAGGCACGCTGGGTCAAGATGTTATTGATATCCGT	86
ORIGINAL	50	aactggatgtgctgaaaggcagctgggtcaagatgttattgatatacgt	99
PCR	87	ACTCTCGSTTCAAAGGTGTGTTACCTTTGACCCAGGCTTCACTTCAAC	136
ORIGINAL	100	actctcggttcaaaagggtgtgttcacctttgaccaggttcaactcaac	149
PCR	137	CGCATCTCGGAATCTAAAATTACTTTTATTGATGGTGATGAAGGTATTT	186
ORIGINAL	150	cgcatacctcgaaatctaaaattacttttattgatggatgaaggtat	199
PCR	187	TGCTGCACCGCGSTTTCCGATCGATCAGCTGGCGACCGATTCTAATACTAC	236
ORIGINAL	200	tgctgcaccggtttcccgatcgatcagctggcgaccgattctaactac	249
PCR	237	CTGGAAGTTTGTACATCCTGCTGAATGGTGAAAAACCGACTCAGGAACA	286
ORIGINAL	250	ctggaagtttgttacatcctgctgaatggtgaaaaaccgactcaggaaca	299
PCR	287	GTATGACGAATTTAAAACFACGGTACCCGTCATACCATGATCCACGAGC	336
ORIGINAL	300	gtatgacgaatttaaaactacggtgaccgctcataccatgatccacgagc	349
PCR	337	AGATTACCCGCTGTTCCATGCTTTCGTCGCGACTCGCATCCAATGGCA	386
ORIGINAL	350	agattaccgctctgttccatgctttcogtccgactcgcataccaatggca	399
PCR	387	GTCATGTGGTATTACCGCGCGCTGGCGGCGTTCCTTTCAGACTCGCT	436
ORIGINAL	400	gtcatgtggattaccgcgcgctggcgggcgttccttcaactcagactcgt	449

**Figure 3.19:** EBI pairwise alignment of NADH insensitive and wild type *cs* gene showing the position of mutation

### 3.3.4 Heterologous overexpression of *E. coli* NADH insensitive *cs* gene in *P. fluorescens* PfO-1

pY146F plasmid transformed in *P. fluorescens* PfO-1 by electroporation. The transformants showed resistance against gentamycin. Restriction enzyme digestion of the isolated plasmid revealed the authenticity of the plasmid (**Fig.3.20**).

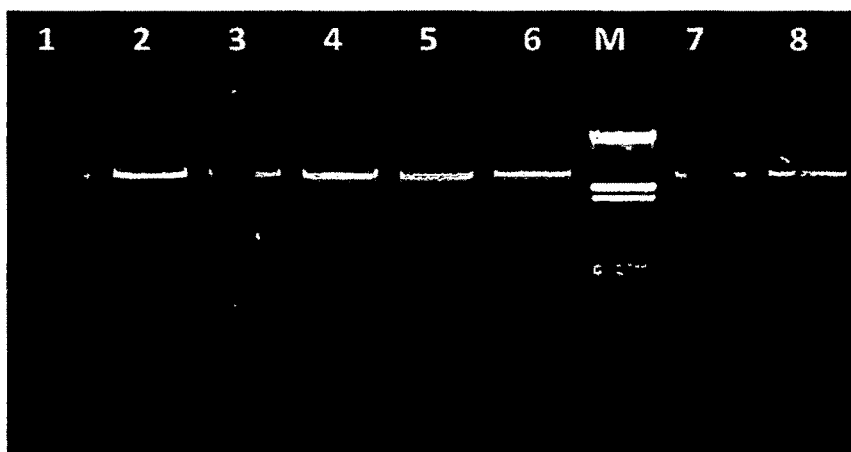
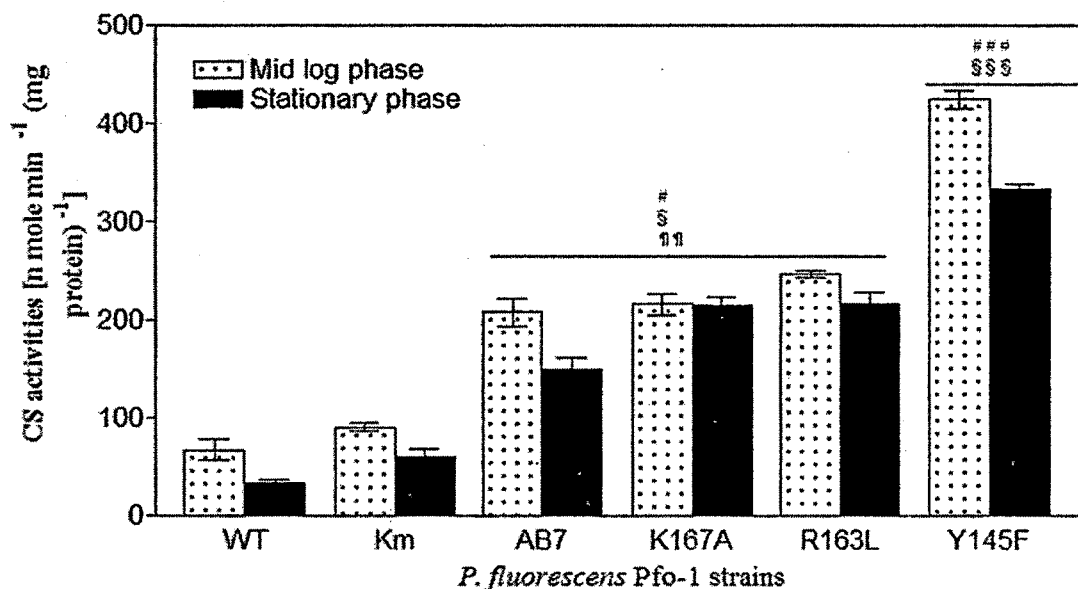


**Figure 3.20: EcoRI-BamHI restriction digestion pattern for pUCPM18 Km<sup>r</sup> containing *E. coli* NADH insensitive *cs* gene from *P. fluorescens* PfO-1 and *P. fluorescens* ATCC13525 transformants. Lane1: *P. fluorescens* PfO-1 with pR163L plasmid (6971,1281bp); Lane2: *P. fluorescens* PfO-1 with pAB8 plasmid (6971 bp); Lane3: *P. fluorescens* ATCC13525 pR163L (6971 ,1281 bp); Lane4: *P. fluorescens* ATCC13525 with pAB (6971 bp); Lane5: *P. fluorescens* PfO-1 with pAB7 (6971,1281 bp); Lane6: *P. fluorescens* ATCC13525 with pAB7(6971, 1281 bp); Lane7: *P. fluorescens* ATCC13525 with Y146F(6971, 1281 bp); Lane8: *P. fluorescens* PfO-1 with Y146F (6971,1281 bp); LaneM: MWM with Lamda DNA *EcoRI*/*HindIII* double digest**

### 3.3.5 Biochemical effects of *E. coli cs* gene overexpression in *P. fluorescens* PfO-1

#### 3.3.5.1 Alterations in citrate synthase activity

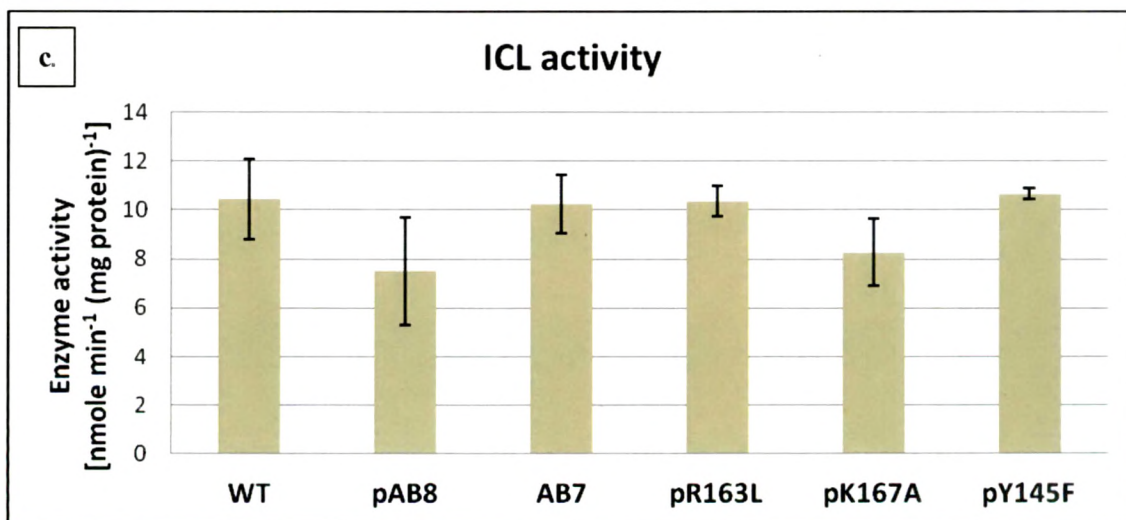
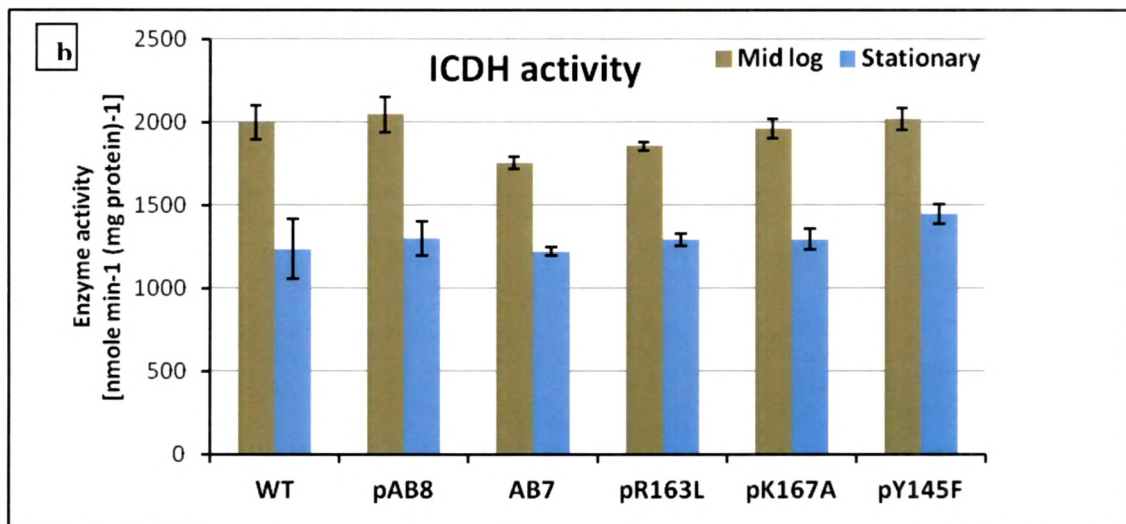
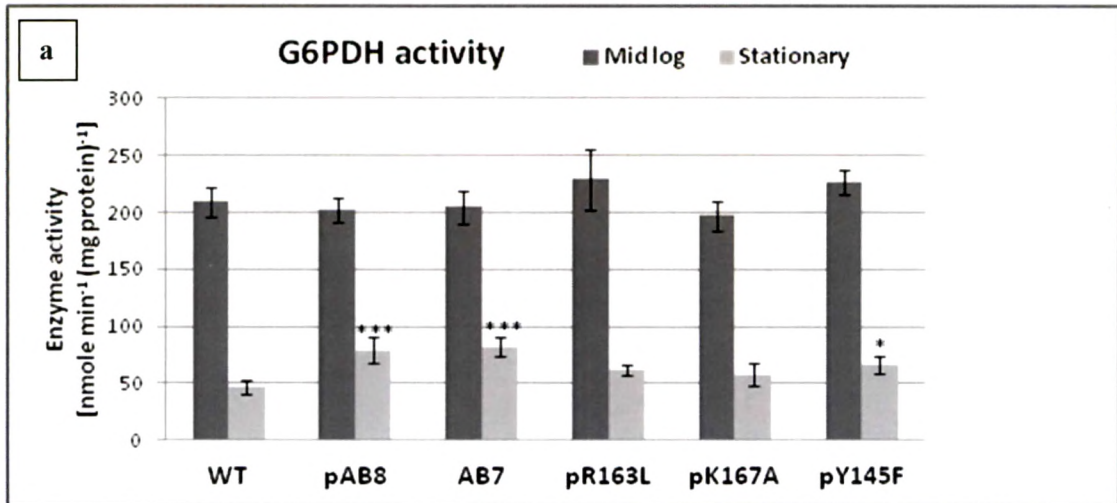
*P. fluorescens* PfO-1 harbouring pY145F showed maximum CS activity of  $424.6 \pm 16.1$ U and  $333.4 \pm 8.5$ U in the mid log and stationary phase, respectively, on M9 minimal medium in the presence of 100 mM glucose which is about 4.7 and 5.6 fold higher than that in the control Pf(pAB8), that showed  $90.3 \pm 6.7$ U and  $60 \pm 14.7$  CS activity respectively. Also Pf(pY145F) showed the highest *cs* activity amongst all the other variants which is 2 fold, 1.7 fold and 1.96 fold higher as compared to the wild type *cs* bearing strain Pf(pAB7) and other two NADH insensitive *cs* bearing strain Pf(pR163L) and Pf(K167A) respectively in the mid log phase (**Fig.3.21**).



**Figure 3.21: Citrate synthase activity of *P. fluorescens* Pfo-1 transformants.** The activity have been estimated using wild type, *Pf*(pAB7), *Pf*(pAB8), *Pf*(pK16A), *Pf*(pR163L) and *Pf*(pY146F) cultures grown on M9 minimal medium with 100mM glucose from mid log phase and stationary phase cultures. Values are represented in the units of nmoles/min/mg total protein. The values are depicted as Mean  $\pm$  S.E.M of 4 independent observations. # Comparison of parameters with respective Wild type, § with respect to Vector control pAB8, ¶ comparison between parameter of pY146F with pAB7,pR163L and pK167A.###, §§§,¶¶¶P<0.001; ##, §§,¶¶P<0.01; #, §,¶P<0.05

### 3.3.5.2 Alterations in G-6-PDH, ICDH, ICL, PYC, and GDH activities

The effect of overexpression is also being monitored at the level of key enzymes of glucose catabolism in both mid log and stationary phase of growth. In *Pf*(pY146F) the periplasmic GDH activity increased by 2.1, 1.4 and 1.26 fold as compared to the wild type, *Pf*(pAB8) and *Pf*(pAB7), respectively, in the stationary phase. There is a significant alteration in GDH activity found in vector control *Pf*(pAB8) as compared to the wild type strain. Similarly a significant increase in PYC activity (2.4, 2.1 and 0.15 fold in the mid log and 6.5, 4.1, 1.7 fold in the stationary phase) was observed as compared to the respective controls. ICL and ICDH activities in both mid log and stationary phase and G6PDH activities in the stationary phase cultures remained unaltered. However in the mid log phase an altered G6PDH activities had increase in activity in *Pf*(pAB8) and *Pf*(pAB7) and significant decrease in *Pf*(pY146F) were monitored as compared to the wild type strain (Fig. 3.22).



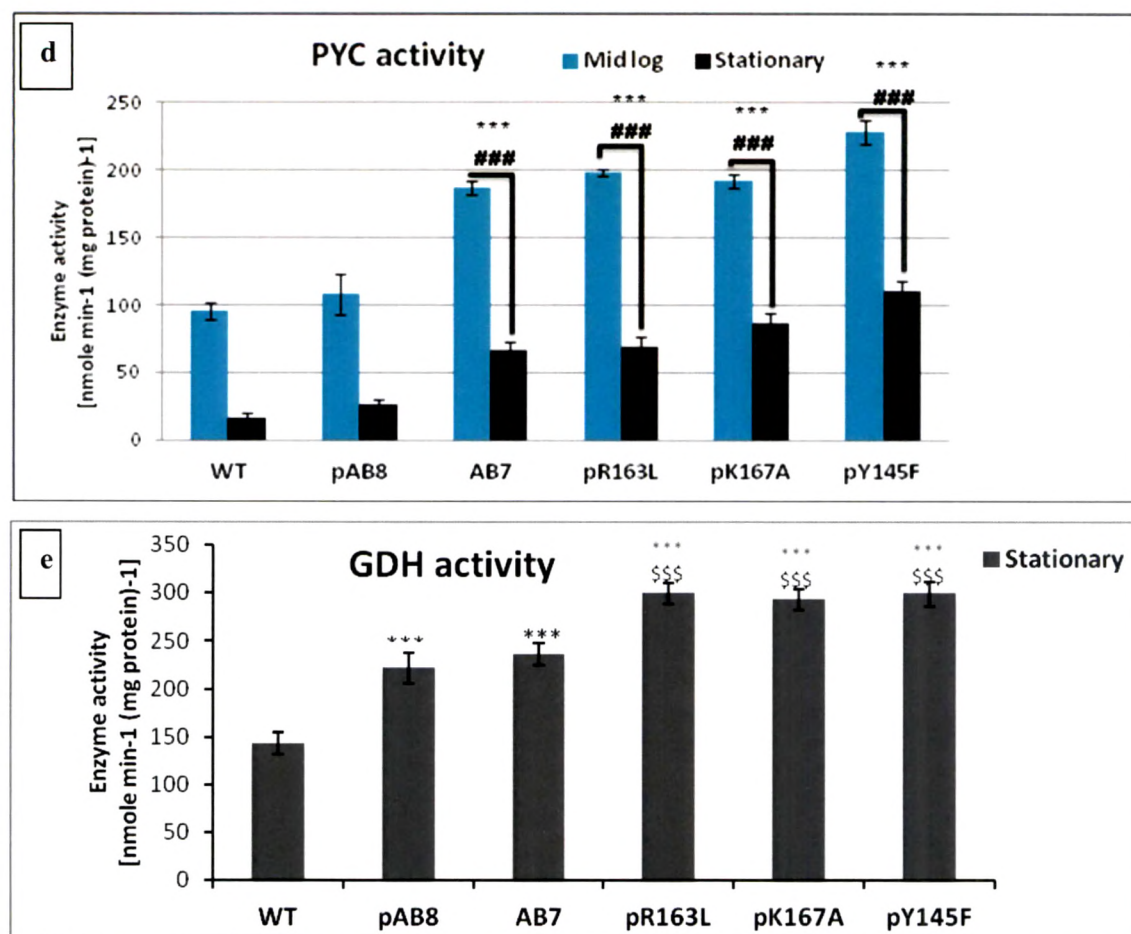


**Figure 3.22: Activities of enzymes G-6-PDH (a) , ICDH (b), ICL (c), PYC (d), and GDH (e) in *P. fluorescens* PFO-1 *cs* transformants.** The activities have been estimated using wild type, *Pf*(pAB7), *Pf* (pAB8), *Pf* (pK16A), *Pf* (pR163L) and *Pf* (pY146F) cultures grown on M9 minimal medium with 100mM glucose. All the enzyme activities were estimated from mid log phase and stationary phase cultures except ICL and GDH which were estimated only in mid log and stationary phase respectively. All the enzyme activities are represented in the units of nmoles/min/mg total protein, . The values are depicted as Mean  $\pm$  S.E.M of 4 (N=4) independent observations. \*Comparison of parameters with respective Wild type; \$ Comparison with respect to pAB8 and ,# comparison between parameters of pY146F with pAB7, pR163L and pK167A.\*\*\*,\$\$\$,###P<0.001; \*\*,,\$\$,##P<0.01; \*,,\$,##P<0.05

### 3.3.5.3 Organic acid secretion

The NADH insensitive *cs* overexpression caused a significant alterations in both intracellular and extracellular citric acid levels and yields. Intracellular citric acid levels in *Pf*(pY146F) increased by 5.7, 6.9 and 2.6 fold while there is a 5, 7.9 and 2.9 fold increase in

The NADH insensitive *cs* overexpression also caused quantitative changes in secretion of gluconic, pyruvic and acetic acid levels. Stationary phase culture supernatants of *Pf* (pY145F) showed 4.4, 3.8 and 1.6 fold increased level of gluconic acid compared to wild type strain, *Pf*(pAB8) and *Pf*(pAB7), respectively (**Fig. 3.24**). On the other hand, pyruvic acid levels in the extracellular medium decreased significantly by 2.54, 2 and 1.4 fold while acetic acid level increased by 2.9, 2.5 and 1.46 fold, respectively, compared to the controls.

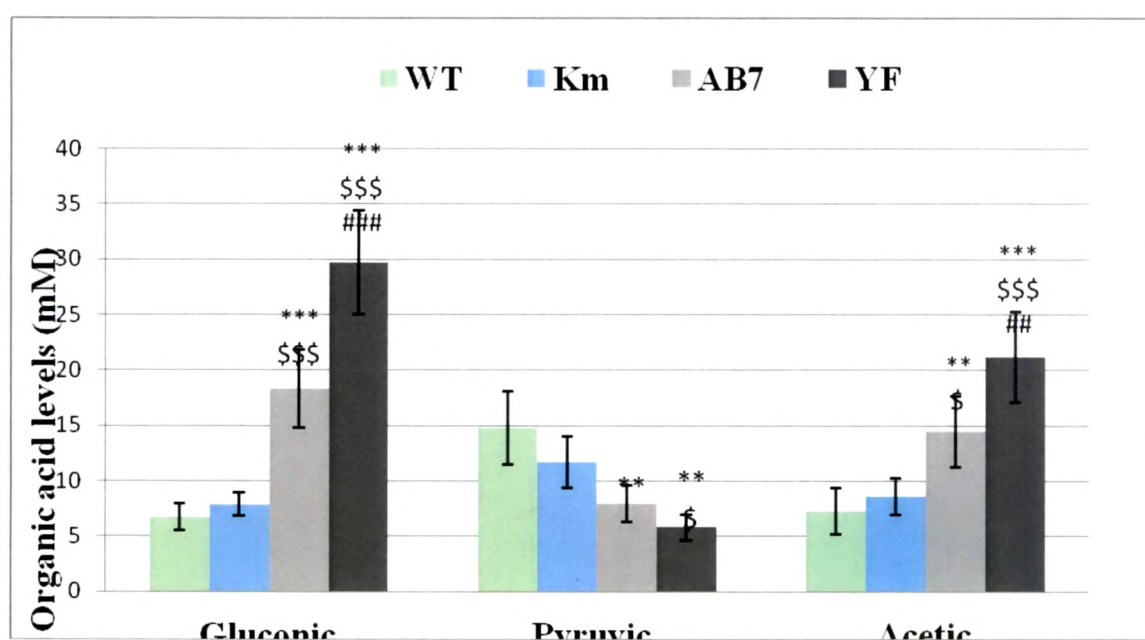


**Figure 3.24: Organic acid secretion from *P. fluorescens* Pf0-1 NADH insensitive *cs* transformants.** Gluconic, pyruvic and acetic acid levels in mM of Wild type, pAB8, pAB7, pYF designated as respective colours in the graph. Parameters estimated from stationary phase cultures grown on M9 medium with 100mM glucose. Results are expressed as Mean  $\pm$  S.E.M of 4 independent observations. \* comparison of parameters with wild type control; \$ comparison of parameters with vector control pAB8, # comparison between parameters of AB7 and YF. \*\*\*, \$\$\$, ### P < 0.001; \*\*, \$\$, ## P < 0.01; \*, \$, # P < 0.05

### 3.3.6 Effect of NADH insensitive *E. coli* *cs* overexpression on growth, biomass and glucose utilization of *P. fluorescens* PfO-1

In the presence of excess glucose, increase in *CS* activity did not significantly affect the growth profile and acidification of the medium within 30 h. However, there is a significant enhancement of pH drop in case of Y146F compared to wild type *cs* bearing strain and other control strain. Specific growth rate, specific total glucose utilization rate and total amount of glucose utilized after 30h remained unaffected. The amount of glucose consumed intracellularly is reduced by 1.49 fold in *Pf*(pY146F) as compared to *Pf*(pAB8). The increase in *CS* activity in *Pf*(pY146F) strain improved the biomass yield by 3.2, 2.38 and 2 fold compared to WT, *Pf*(pAB8) and *Pf*(pAB7), respectively (**Table 3.5, Fig. 3.25**).

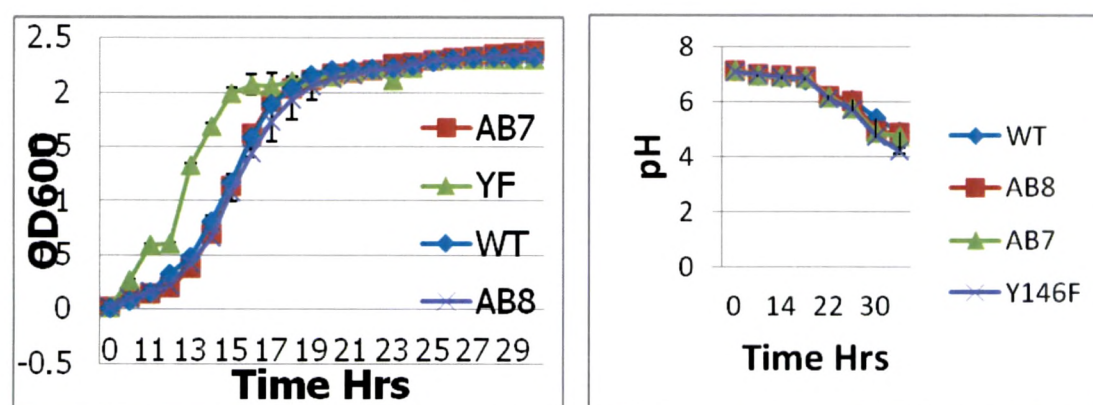


Figure 3.25: Growth and pH profiles of *P. fluorescens* PfO-1 *cs* transformants on M9 minimal medium with 100mM glucose. The values plotted represent the Mean $\pm$ S.D of 4-6 independent observations.

Table 3.5: Physiological variables and metabolic data from *P. fluorescens* Pf0-1 *cs* transformants grown on M9 medium with 100mM glucose

Bacterial strain	Sp. Growth rate $\mu(\text{h}^{-1})^{\dagger}$	Total glucose utilized(mM) $^{\ddagger}$	Glucose consumed (mM) $^{\ddagger}$	Biomass yield $Y_{\text{dcw}/\text{Glc}}^{\dagger}$ ( $\text{g g}^{-1}$ )	Sp. Glucose utilization rate $\text{QGlc}^{\dagger}$ [ $\text{g}(\text{g dcw})^{-1} \text{h}^{-1}$ ]
WT	0.42 $\pm$ 0.03	50.45 $\pm$ 7.08	45.94 $\pm$ 6.62	0.12 $\pm$ 0.02	4.5 $\pm$ 0.55
<i>Pf</i> (pAB8)	0.59 $\pm$ 0.04	69.88 $\pm$ 9.4	62.22 $\pm$ 8.5	0.16 $\pm$ 0.03	7.20 $\pm$ 1.3

<i>Pf</i> (pAB7)	0.65 ± 0.04	65.86 ± 4.86	48.6 ± 3.57	0.19± 0.04	6.35 ± 1.56
<i>Pf</i> (pY145F)	0.61±0.06	71.46±6.7	41.71±5.75\$\$\$	0.38±0.01\$\$\$	6.8±1.03

. The results are expressed as Mean ± S.E.M of readings from 4-6 independent observations. † Biomass yield (Y<sub>dcw</sub>/Glc), specific growth rate ( $\mu$ ) and specific glucose consumption rate (QGlc) were determined from the mid-log phase of each experiment. ‡ Total glucose consumed and glucose utilized were determined at the time of pH drop (30h) for *Pf* (Y146F), *Pf* (pAB7) and *Pf* (pAB8) \*Comparison of parameters with respective wild type; \$ Comparison of parameters with *Pf* (pAB8) and # comparison between parameters of pY146F and pAB7. .\*\*\*,\$\$\$,###P<0.001; \*\*,\$\$,##P<0.01; \*,\$,#P<0.05

### 3.4 DISCUSSION

Present study demonstrates the effect of overexpression of NADH insensitive *E. coli* *cs* in metabolically distinct *P. fluorescens* PfO-1. Three *E. coli* NADH insensitive *cs* R163L, K167A and Y145F when constitutively overexpressed under *lac* promoter in *P. fluorescens* PfO-1, a maximum of 5.6 fold and 2 fold overexpression was obtained in *Pf* (Y145F) as compared to the control and strain bearing the wild type *cs* gene. Our data is supported by a study of Duckworth et al., (2003) which showed maximum weakening of NADH binding in case of Y145F. The study carried out in *E. coli* K12 strain showed  $K_i$  value of 790 ±210  $\mu$ M for Y145F as against wild type *cs* with a  $K_i$  value of 2.8 ±0.4  $\mu$ M for 100 percent inhibition by NADH (Table.3.2) which clearly indicates weakening of NADH binding to the active site and enhancement of CS activity.

In our earlier work when *E. coli* wild type *cs* gene was constitutively overexpressed under *lac* promoter in *P. fluorescens* ATCC 13525 a 2 fold enhanced activity was observed compared to the control strain (Buch et al., 2009). In the present study, as a consequence of 5.6 fold increase in CS activity in *Pf* (pY145F) there is a 6.9 fold elevated intracellular citrate level which is accompanied by 51.6 and 29.6 fold enhancement of extracellular citrate levels and yields. Remarkably the high citrate accumulation in *Pf* (pY145F) had no effect on growth. This pattern of accumulation of intracellular citric acid was similar to *P. fluorescens* ATCC13525 overexpressing *E. coli* wild type *cs* gene in which 2 fold increase in CS activity lead to 2 fold elevated intracellular citrate level and 26 fold enhancement of

extracellular citrate yield (Buch et al., 2009). In another study *icd* mutant of *E. coli* K and B strains resulted in an increase of ~3.8 and 2.5 fold CS activity and enhanced citrate accumulation but unlike our study, in this case citrate accumulation had a negative effect on growth of the *E. coli* strains (Aoshima et al., 2003). Overexpression of mitochondrial CS genes also resulted in increased citrate efflux in cultured carrot cells (Koyama et al. 1999), Arabidopsis (Koyama et al. 2000), and canola (Anoop et al. 2003) plants

Increase in intracellular citrate level and yield by 1.9 and 2.39 fold, respectively, in *Pf*(pY145F) compared to *Pf*(pAB7) does not lead to similar increase in extracellular citrate levels. Citric acid being the substrate of central carbon metabolism must be transported into and out of the cell for efficient bioactivity. Therefore low level of extracellular citrate can be attributed to weak efflux transport mechanism in *P. fluorescens*. The transport of citric acid in gram negative bacteria is mediated by hydroxycarboxylate transporters which are a family of secondary transporter. These transporters are either H<sup>+</sup> or Na<sup>+</sup> symporters or they catalyze exchange between two substrates. (Lolkema and Sobczak, 2005). From database it is clear that the citrate transport in fluorescent pseudomonads is H<sup>+</sup> dependent. The low efficiency of the native citrate transport can be attributed to the low intracellular proton concentration compared to the outer membrane proton concentration. The active transport system for citrate excretion also appears to be the main rate-determining factor in citrate overproduction by yeasts (Anastassiadis and Rehm, 2005) while in addition to citrate export, transport of sugar and ammonia into the cell are also crucial for citric acid production by *A. niger* (Papagianni, 2007).

Increased gluconic acid levels with simultaneous reduction in pyruvic acid levels could be explained by increased PYC activity in *Pf*(pY145F), which could probably divert pyruvate flux towards increased OAA biosynthesis to meet the increased CS activity. Even in *A. niger* the enhancement of anaplerotic reactions replenishing TCA cycle intermediates predisposes the cells to form high amounts of citric acid (Legisa and Matthey, 2007). However, *cs* overexpression in *A. niger* did not affect PYC activity (Ruijter et al., 2000). Enhancement of biosynthetic reactions due to shortage of TCA cycle intermediates was also observed in citric acid accumulating *E. coli* K and B strains in the form of increased glyoxylate pathway (Aoshima et al., 2003; Kabir and Shimizu, 2004). However, similar

increase in flux through glyoxylate shunt was not apparent in *Pf* (pY145F) as evident from very low and unaltered ICL activity detected in *Pf* (pAB8) and *Pf* (pY145F). Low ICL activity was consistent with earlier reports in *P. fluorescens* ATCC13525 and *P. indigofera* in which ICL contributed negligibly to glucose metabolism (Buch et al., 2009; Diaz-Perez et al., 2007).

The phosphoenolpyruvate carboxylase reaction and the glyoxylate shunt are utilized for the supply of oxaloacetate to the TCA cycle. The glyoxylate shunt contributes to supplying oxaloacetate via glyoxylate, succinate, fumarate and malate by using isocitrate in the TCA cycle and acetyl-CoA which is produced by acetate catabolism. Our experimental results using the *cs* overexpression strain suggest that *P. fluorescens* PfO-1 might use the phosphoenolpyruvate carboxylase rather than the glyoxylate shunt reaction for maintaining intracellular oxaloacetate levels to adapt to the higher OAA demand which is supported by the increase in acetate production in *Pf* (pY145F) compared to the control. Enhanced CS activity in *Pf* (PY145F) also increased the periplasmic glucose oxidation which is reflected by increase in GDH activity and gluconic acid production. Moreover, significant decrease in glucose consumption without affecting the glucose utilization suggested the involvement of direct oxidation pathway for carbon flux distribution in *P. fluorescens*. The increased carbon flow through glycolysis led to increased protein synthesis that is reflected to increased biomass. The citrate induced oligosaccharide synthesis was reported in *Agrobacterium* sp. ATCC 31749 (Ruffing et al., 2011)

The central carbon metabolism network gets to the heterologous overexpression of NADH insensitive *E. coli cs* in *P. fluorescens* PfO-1 (**Fig. 3.26**). The conditions created in the present work include: improvement of glucose uptake, improvement of CS activity and citrate production compared to the earlier report by Buch et al. (2003), suppression of pyruvate secretion and enhanced acetate production, increased direct oxidation of glucose leading to more gluconate production.

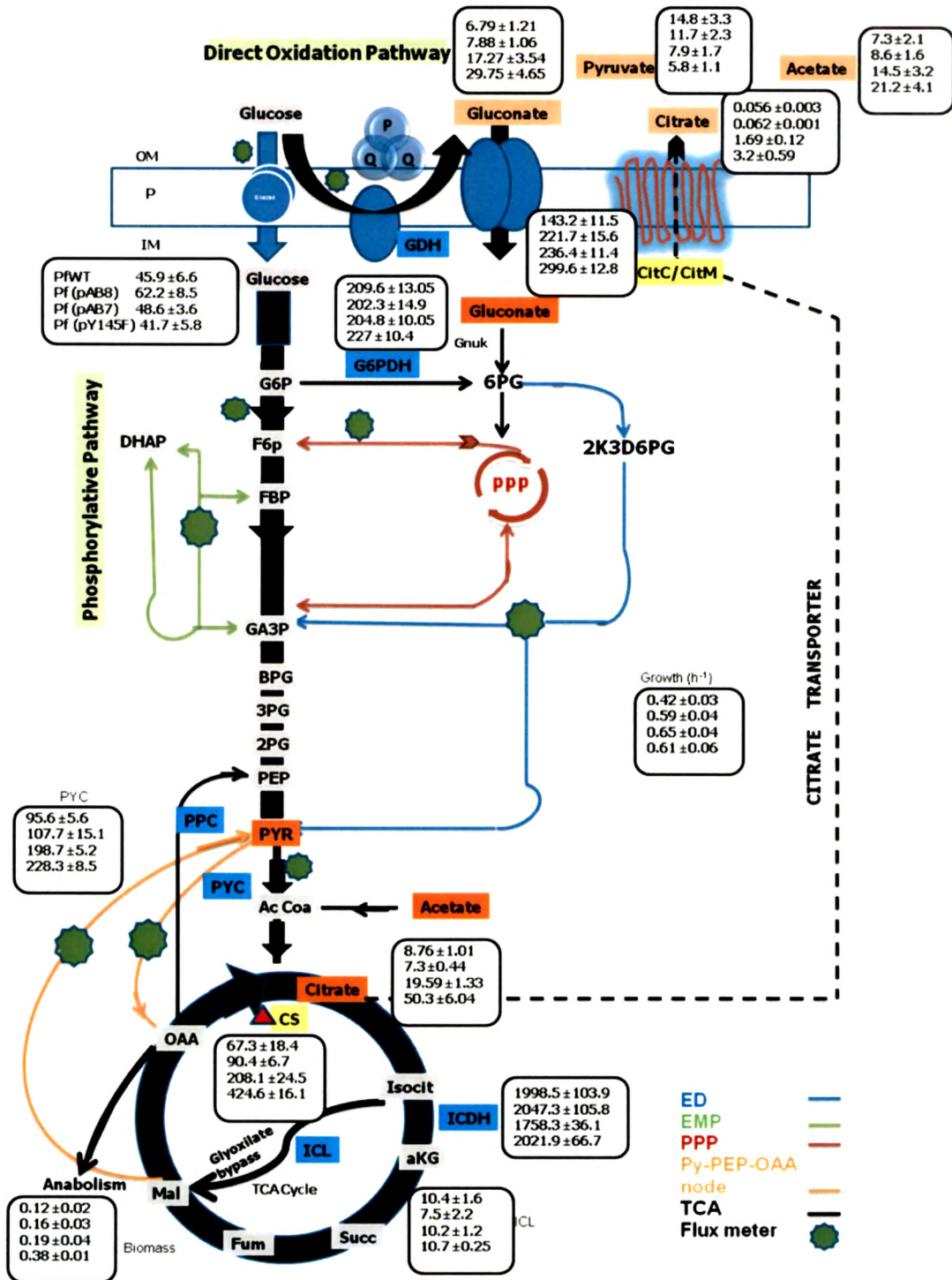


Figure 3.26: Key metabolic fluctuations in *P. fluorescens* PFO-1 overexpressing NADH insensitive *E. coli* CS